Application of a Generalised Enthalpy–Entropy Relationship to Binding Co-operativity and Weak Associations in Solution

Mark S. Searle, Martin S. Westwell and Dudley H. Williams*
Cambridge Centre for Molecular Recognition, University Chemical Laboratories, Lensfield Road, Cambridge, UK CB2 1EW

Enthalpy–entropy compensations are a consequence of weak associations where the binding enthalpy is much lower than typical covalent bond strengths. The general form of an enthalpy–entropy curve is presented based upon theoretical considerations and justified on the basis of experimental data for associations in the gas phase and for monatomic sublimation. The intrinsic curvature of the enthalpy *vs.* entropy plot provides the basis for a description of co-operativity and binding phenomena in solution. In the case of cooperativity, we divide the mutual aiding of two interactions into two distinct parts, one of which is entropic in origin and related to the classical chelate enhancement of binding of Jencks; the other is an enthalpic benefit due to improved electrostatic bonding. Since the experimental Gibbs energy for all weak associations in solution is a consequence of competing solute–solvent, solvent–solvent and solute–solute interactions, the summation of these interactions can be usefully described by a vector analysis using the enthalpy–entropy curve. We illustrate the utility of this approach by presenting a qualitative description of the various contributions to binding in the following examples: (*i*) one-point associations in non-polar solvents, (*ii*) entropy-driven association of two large discs involving the release of multiple solvent molecules and (*iii*) enthalpy driven associations involving metal chelation by polyamines. By considering the curvature of the enthalpy–entropy plot for a given interaction, in combination with the possibility of making or breaking multiple interactions on one template, net enthalpies and entropies of association in solution can be explored in an approximate manner.

The prediction of binding constants for weak interactions in solution has remained an elusive goal. The goal is of course one of importance in view of the desire to place molecular recognition on a firm numerical footing and to understand the molecular basis of biology. For an association of two solute molecules A and B to give a complex A.B, there is an entropic cost as a consequence of degrees of freedom of motion lost when the associating entities are constrained within the complex. When the degree of constraint is such that an essentially 'rigid' complex is formed in which there is no relative motion between A and B (such as is the case when A and B are connected by a covalent bond), then the price in entropy for the association approaches its limiting value of 50–60 kJ mol^{-1} ($T\Delta S°$ at 298 K), for molecules of low molecular mass (100–300 Da).[1] In some approaches to the study of weak interactions (*i.e.* where the A.B bond strength is much lower than that of a covalent bond), a similar entropic cost is assumed,[2,3] and residual motion of the complex is then allowed for in terms of the favourable entropy of new soft vibrations in the complex.[3] However, this approach gives rise to anomalously large hydrogen bond strengths.[3] A better approach[4] appears to be that in which the entropic cost ($T\Delta S°$ at 298 K) of the association of A and B is some fraction of 50–60 kJ mol^{-1},[1,5,6] and is a sensitive function of the exothermicity of the interaction,[4,7] such that an increasing enthalpic benefit of bonding is offset by an increasing adverse entropy of restricted motion. This phenomenon of enthalpy–entropy compensation is of fundamental importance to molecular associations in situations where the binding enthalpy is comparable to, or even many times, the thermal energy RT (where R is the gas constant and T the temperature; $RT \approx 2.5$ kJ mol^{-1} at 298 K), but of lesser importance at typical covalent bond strengths.[7] The origin of the phenomenon is to be found in the depth of the electrostatic well, corresponding to the associated state, and in the density of states within the well, as illustrated in Fig. 1. When the associated state A.B lies in a deep electrostatic well [with $\Delta H°$ perhaps > $40RT$; Fig. 1(*a*)],

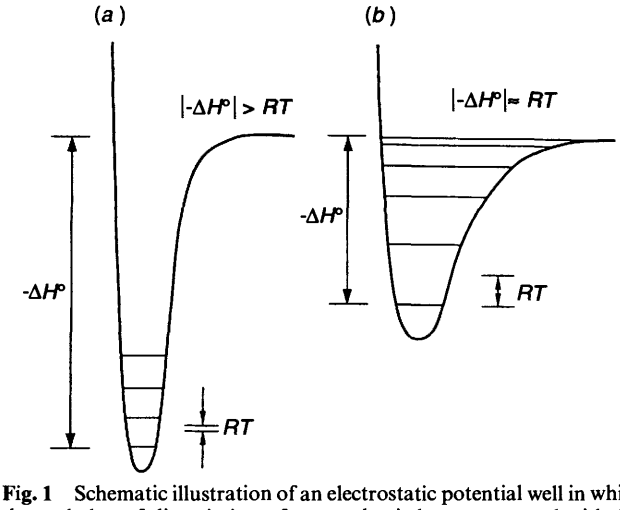

Fig. 1 Schematic illustration of an electrostatic potential well in which the enthalpy of dissociation of a complex is large compared with RT (thermal energy at room temperature) (*a*) and where the enthalpic barrier to dissociation is comparable to, or several times, RT (*b*)

relatively little motion is permitted compared with the dissociated state in which the electrostatic attractions between A and B are removed. Conversely, associated states that occupy more shallow wells [say $\Delta H° < 10RT$; Fig. 1(*b*)] have much residual motion since energy levels corresponding to large amplitude vibrations close to the lip of the well (where the density of states is also greatest) will be more highly populated than when the well is deep [Fig. 1(*a*)].[7] From these arguments, it can be seen that 'sloppy' associations with very small exothermicities can give rise to remarkably small losses of entropy, but also that the limiting entropy, corresponding to the maximum possible loss of motion is only likely to be achieved in the case of very large binding exothermicities that

may well lie outside the range possible for complexes formed through weak, non-covalent interactions.[8]

Many recent thermodynamic studies have highlighted the linear relationship between the enthalpy of association ($\Delta H°$) and the corresponding entropy change ($\Delta S°$), particularly in host–guest recognition. Examples include complexation of cationic species with synthetic and natural hosts such as glymes–podands, crown ethers, cryptands, bis(crown ethers) and ionophore antibiotics.[9–12] Similar relationships are found in the extraction of metal picrates by crown ethers,[13,14] in the inclusion complexation of cyclodextrins in water,[15] the molecular recognition of quinones through interaction with porphyrins,[16] the formation of cyclophane–arene inclusion complexes[17] and in stability studies of many types of nucleic acid structure in water.[18] Examples of linear relationships in biological recognition studies have also been highlighted for the binding of nucleotides to ribonuclease,[19] flavin analogues to riboflavin binding protein[20] and in protein catalysis.[21] The slope of the relationship between $\Delta H°$ and $T\Delta S°$ from host–guest recognition studies has been proposed to be characteristic of host topology and complex stoichiometry and a measure of the extent of desolvation caused by complexation,[15] although the origins of the effect have not been addressed. Previous explanations have been sought to explain these linear relationships.[22–25] For example, transition-state theory has been used to relate the compensation effect to a dependence of the entropy change on the activation energy for formation of the transition state.[22] In studies of heterogeneous catalysis[23] the effect was credited to specific surface properties. Linert and Jameson have recently reviewed the 'isokinetic relationship'[24] and concluded that the effect is a natural outcome of the interplay between solvent and system; others have also concluded that the compensation effect can be explained in terms of some unique property of solvent (water).[25] In summary, a unifying description has not emerged. We emphasize that enthalpy–entropy compensations are a general consequence of all weak interactions (as described above with reference to Fig. 1) and are manifested in solution associations, rather than finding their origin in some unique feature of solvation.

In this paper we present the general form of an enthalpy–entropy compensation curve based upon theoretical considerations and experimental data. The generalized shape of the curve is justified on the basis of experimental measurements for associations in the gas phase and for monatomic sublimation, and provides the basis for a useful (although, at this stage qualitative) description of binding phenomena in solution. The experimental Gibbs energy for weak associations in solution is analysed as a consequence of competing solute–solute, solute–solvent and solvent–solvent interactions. Each interaction is described by a point on an enthalpy–entropy compensation plot. We introduce a vector analysis to illustrate the application of this generalized curve in summing the various interactions that contribute to the net $\Delta G°$, $\Delta H°$ and $T\Delta S°$ for an association.*

Discussion

A Generalized Enthalpy–Entropy Compensation Plot.—There is a limit to the adverse entropy of a bimolecular association

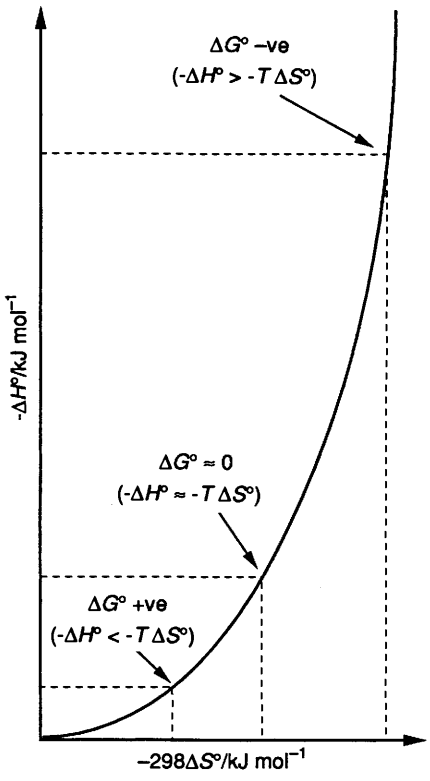

Fig. 2 The general form of the extent of the exothermicity of association ($\Delta H°$) A + B ⟶ A.B as a function of the entropic cost ($\Delta S°$) at a temperature T. There is a limit in the price in entropy to be paid (essentially due to loss of translational and rotational freedom) and this limit is approached before limiting bond strengths are approached.

(*ca.* 50–60 kJ mol^{-1} for $T\Delta S°$ in solution at 298 K), yet the exothermicity of an interaction can increase far beyond the exothermicity at which the limiting cost in entropy is approached. Hence we propose (and subsequently justify) that the enthalpic benefit *vs.* entropic cost of an association will be of the general form shown in Fig. 2. For very weak associations, the equilibrium constant may be less than one ($\Delta G°$ +ve); the entropic cost is greater than the enthalpic benefit. For example, the association of an Ar atom with a Kr atom has been studied at low temperature (T < 120 K) giving $\Delta H° = -2.6$ kJ mol^{-1} and $\Delta S° = -48.5$ J K^{-1} mol^{-1}, with $\Delta G° = +3.2$ kJ mol^{-1} at 120 K.[26] At 298 K, $\Delta G°$ would have an even more positive value (*cf.* Fig. 2), making association insignificant. As the exothermicity in Fig. 2 increases, $\Delta G°$ passes through zero and then gradually becomes increasingly negative (the enthalpic benefit will be much greater than the entropic cost), reaching the limiting entropy value. The latter situation is reached in the case of monatomic sublimation (Fig. 3);[27] only translational entropy is gained in passing from the solid to vapour, reaching a limiting value of *ca.* 45 kJ mol^{-1} at 298 K, which is mass (m) independent to a useful approximation, since translational entropy depends on the logarithm of $m^{3/2}$.[28] Limiting entropy changes for bimolecular associations in the gas phase are similarly illustrated for homolytic pyrolysis of hydrocarbons. For C–C bond cleavage a limiting entropy change of *ca.* 60 kJ mol^{-1} is observed at 298 K, representing a gain in both translational and rotational entropy for both radicals.[29] A collection of sublimation data and gas-phase association data recorded at close to 298 K (Fig. 4) indicates qualitatively the direction of the anticipated curvature from a diverse set of experiments.[30–33] This trend is clear despite the enormous variety of systems for which data has been collated.

Despite the evidence for curvature in enthalpy–entropy plots

* We use standard state thermodynamic quantities $\Delta G°$, $\Delta H°$ and $\Delta S°$ throughout: for solids, liquids and gases the standard state corresponds to the pure substance at 1 atm and 298 K (1 atm = 101 325 Pa). For aqueous solutions the standard state corresponds to an ideal solution of unit molarity at 1 atm and 298 K. Thus, for an association A + B ⟶ A.B in aqueous solution at 298 K, $\Delta G°$ is the change in Gibbs energy when the complex A.B is formed from A and B present in 1 mol concentration prior to association.

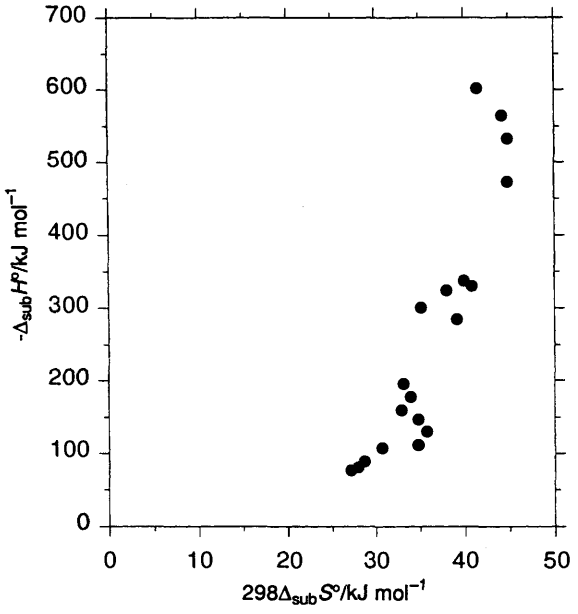

Fig. 3 Enthalpy of sublimation *vs.* entropy of sublimation for monatomic elements

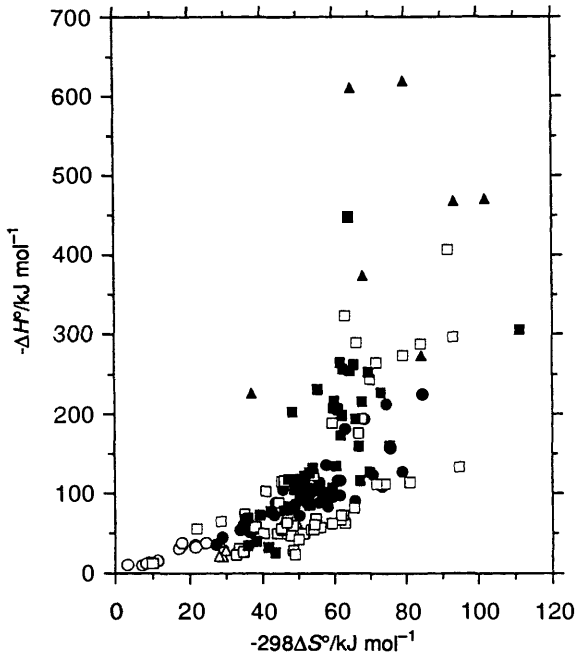

Fig. 4 Enthalpy ($\Delta H°$) *vs.* entropy ($298\Delta S°$) plot for gas phase associations. Key: ○ complexation of iodine (I_2) with donor molecules, *e.g.* benzene, diethyl ether; ● sublimation of organic molecules; ■ sublimation of ionic crystals; ▲ sublimation of oxides; □ sublimation of inorganic molecular crystals; △ association of HF with base, *e.g.* HCN. All of the system cited involve small or negligible changes in internal rotations upon association.

(Figs. 3 and 4), experimental data for solution interactions from various laboratories,[9–25] and as also presented below (Fig. 5), show approximately linear relationships between $\Delta H°$ and $T\Delta S°$ for weak associations in non-polar solutions. How then do we reconcile these linear plots with the general form of an enthalpy–entropy compensation plot that is curved? In using experimental data from solution studies there is inevitably discrimination against associations which involve very large negative Gibbs energy changes because of the difficulties of measuring large equilibrium constants, $K > 10^8$ dm^3 mol^{-1}. Also, the fundamental relationship between $\Delta H°$ and $\Delta S°$ may be partially obscured by the fact that each experimental point

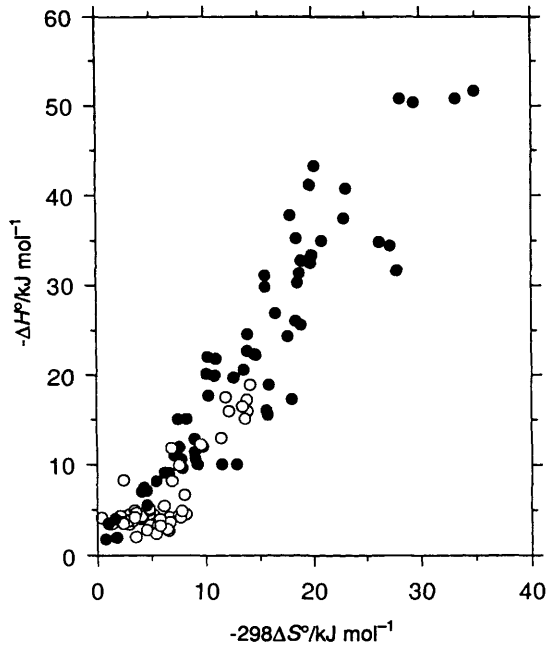

Fig. 5 Enthalpy ($\Delta H°$) *vs.* entropy ($298\Delta S°$) plot of experimental data for 'one-point' associations in non-polar solvents. Data include charge transfer complexes of iodine (●) and collision complexes (○) corresponding to weak (non-covalent) interactions.

is a composite of interactions involving solvent and solute, as described in detail below. In earlier work,[4] we used sublimation data to illustrate the linear relationship between bonding ($\Delta H°$) and dynamics ($\Delta S°$), but of course these data also reflect the similar limitations in measuring very small equilibrium constants. Since data are obtained from temperature-dependent changes in vapour pressure, detectable amounts of vapour of relatively involatile materials (*i.e.* where $\Delta G°$ for sublimation is very large and positive at 298 K) are obtained only when equilibrium constants are brought into an accessible range by making measurements at elevated temperatures. The consequence of heat capacity (associated principally with translational, rotational and vibrational modes in the solid) is that bonding in the crystal is compromised by the benefit of more entropy as the temperature is raised. However, the change in enthalpy and entropy have different dependencies on temperature [eqns. (1) and (2)]; where $\Delta C_p°$ is the change in heat

$$\Delta H° = \Delta C_p°(T_2 - T_1) \quad (1)$$

$$\Delta S° = \Delta C_p° \ln[T_2/T_1] \quad (2)$$

capacity at constant pressure and T_1 and T_2 define a temperature range of interest. Thus, although enthalpy and entropy are compensating there is not a linear relationship between the two. Consequently, ΔH and ΔS for sublimation at higher temperatures must be correspondingly smaller than measured at close to 298 K but by amounts which also result in less positive ΔG values for sublimation. The net effect appears to negate the intrinsic curvature of the relationship between $\Delta H°$ and $\Delta S°$.*

* This would appear to be the case for sublimation of the polar compounds with large $\Delta_{sub}H$ values highlighted in the top right-hand portion of the plot in Fig. 5 of our earlier paper.[4] For example, pyrrole-2-carboxylic acid, 2-furoic acid, benzanthrone, 4-hydroxybenzoic acid and anthracene were studied at elevated temperatures. Since the experimentalists elevated the temperature in order to make $\Delta_{sub}G$ less positive (*i.e.* to give measurable K), then it is required that $\Delta_{sub}H$ is reduced more than $T\Delta_{sub}S$ in the relevant temperature range.

Although the principles which allow the derivation of Fig. 2 have long been established, so far as we are aware, curves of this form have not previously been presented or utilized. We emphasize that it is the general form of Fig. 2 which is useful and are aware that it is an approximation; the precise cost in entropy of an association will also be a function of specific variables such as the mass, density of states and the shape of the potential energy well in which the associated species lies. Further, if more complex associations are considered where the possibility arises that internal rotations are restricted within the associating species, then the limiting entropy change will be displaced to the right in Fig. 2, reflecting a higher limiting entropic cost to the association. For this reason, the entropy axis on Fig. 2 is taken to imply only the loss of translational and overall rotational freedom. Loss of entropy due to the restriction of internal rotations would have to be considered separately.

We first illustrate the importance of the variable slope of the enthalpy–entropy curve in providing a basis for co-operativity in binding phenomena. We describe how two weak interactions, acting to simultaneously support the binding of one molecule to a receptor, produce a net binding energy which is greater than the sum of the parts. In outlining this description, we divide this mutual aiding of the two interactions into two distinct parts; one is entropic in origin and related to the classical chelate enhancement of binding described by Jencks;[5,6] the other is an enthalpic benefit.[34]

Co-operativity in Binding.—We consider a model for binding based upon the consideration of an interaction of a polar functional group in a molecule X with a complementary polar group on a receptor, and of a polar functional group Y with another polar group on the same receptor, as would occur in a gas-phase environment. These interactions are considered when X and Y interact separately with the receptor [Scheme 1(*a*)], or

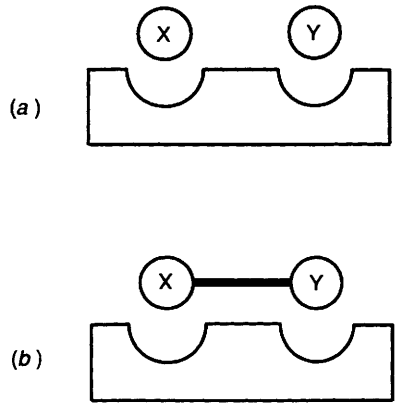

Scheme 1

simultaneously by virtue of being covalently connected together [Scheme 1(*b*)] such that X and Y are able to bind into their respective binding sites without strain and without any adverse entropy change needed to conformationally restrict the connection. We again emphasize that the entropy–enthalpy plot allows a crude guideline to the entropic cost as a function of the strength of the electrostatic interaction formed and that the overall curvature of the plot allows us to make some advances from Jencks' classic analysis of the chelate effect.[5,6] The following cases are now considered.

Exothermicity of binding X–Y is approximately the sum of the exothermicities of X and Y. Suppose molecule X alone binds to the receptor with an exothermicity $\Delta H°_X$ and Y with an exothermicity $\Delta H°_Y$; on the basis of Fig. 2, the respective adverse entropy terms would be $T\Delta S°_X$ and $T\Delta S°_Y$. If the initial assumption is made that X and Y bind with the same exothermicities when separate as when binding to the receptor jointly as X–Y, then the exothermicity of binding X–Y is taken as $\Delta H°_{X-Y}$ and the cost due to loss of translational and rotational entropy ($T\Delta S°_{T+R}$) is $T\Delta S°_{X-Y}$. Thus, in the case of X binding with a relatively small exothermicity, and Y binding with a moderate exothermicity, the enhancement in binding constant for X–Y relative to the sum of the separate components is given by the difference in the entropic cost to binding $T\Delta S°_{X-Y} - (T\Delta S°_X + T\Delta S°_Y)$. In Fig. 6(*a*), each binding interaction (X, Y and X–Y) is represented by a vector from the origin to the relevant point on the entropy–enthalpy curve, with dotted lines identifying the pertinent values for $\Delta H°$ and $T\Delta S°$ for each interaction. In Fig. 6(*b*), the vectors for binding X and Y separately are summed such that overall $\Delta H°_X + \Delta H°_Y = \Delta H°_{X-Y}$, but the difference in $T\Delta S°$ for binding X–Y *versus* the sum for X and Y alone represents the classical chelate enhancement ($T\Delta S°_{chelate}$). Whatever a more precise form of Fig. 2 may be, given only the generality that more exothermic interactions approach a limiting cost in entropy, it is seen that this expression of co-operativity is greatest where each of the associations of X and Y are sufficiently exothermic to approach the limiting cost in entropy [Fig. 6(*c*)]. There are many intramolecular model reactions that exhibit rate increases of between $\approx 10^5$ and $\approx 10^8$, compared with the corresponding bimolecular reactions, where the reacting groups have the freedom to undergo independent translation and rotation and are described in Jencks' classic papers.[5,6] Here, of course, the large adverse entropy involved in forming the transition state in a bimolecular association is largely negated in the intramolecular reaction by a strongly exothermic interaction between the two reacting species that holds them in close proximity, namely a covalent bond. Conversely, when X and Y bind with very small exothermicities, then the chelate effect may be small because the entropic cost of binding X–Y will not be much less than the sum of the entropic cost of binding X and Y separately. This effect arises because of the large change in slope of Fig. 2 on passing from small to large exothermicities.

We next consider the case where co-operativity is also expressed as an enthalpic benefit when X and Y are tethered together in X–Y. This effect operates in addition to the entropic chelate effect just described.

Exothermicity of binding X–Y is greater than the sum for binding X and Y. For each of the interactions of X and Y with the receptor, in general only part of the theoretical maximum translational and rotational entropy which could be lost is lost because in a weak interaction the theoretical maximum bonding (which could only be expressed at 0 K) is not attained at room temperature owing to the opposing entropic advantage of residual motion. The result is that each molecule binds and occupies an average position in the enthalpic well corresponding to $\Delta H°_X$ when X binds alone and $\Delta H°_Y$ when Y binds alone. However, if the restriction of motion is aided by a neighbouring exothermic interaction, then the average position in the enthalpic well will correspond to some larger exothermicity. Thus, the binding of the X part of X–Y is aided by the binding of the Y part of X–Y and *vice versa*, as a consequence of an increased barrier to dissociation of X when X is directly bonded to Y. Therefore, in the general case it is to be expected that the exothermicity of binding X–Y will be greater than the sum of the exothermicities of X and Y alone. The effect of this second co-operative factor, which is quite distinct from the entropic chelate effect described above, is illustrated in Fig. 7. The dotted lines represent the enthalpies of association of X, Y and X–Y ($\Delta H°_X$, $\Delta H°_Y$ and $\Delta H°_{X-Y}$, respectively) which were analysed above with the assumption that $\Delta H°_{X-Y} = \Delta H°_X + \Delta H°_Y$. The dashed lines indicate the corresponding analysis for which X–Y binds more exothermically than the

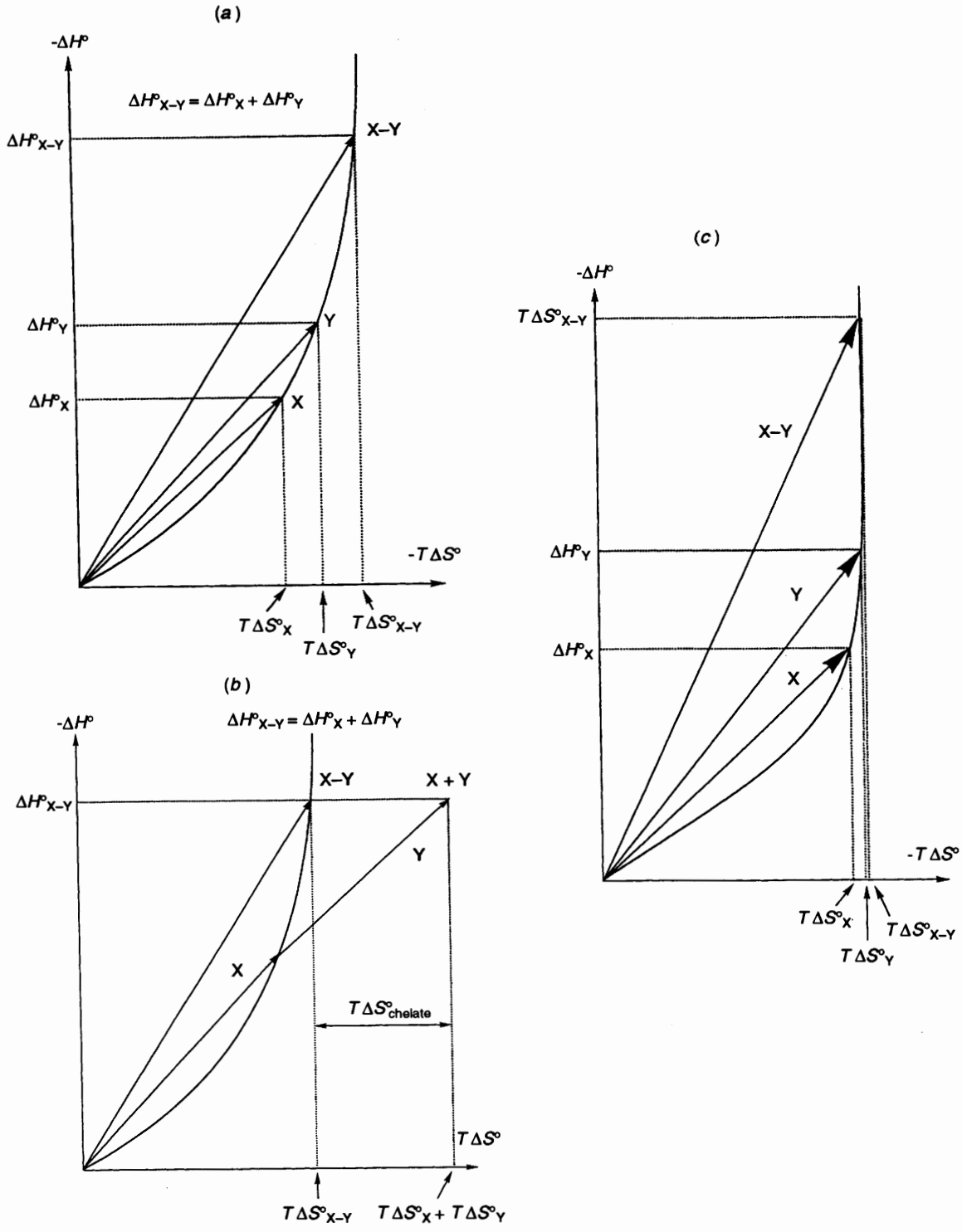

Fig. 6 Vector diagrams describing (*a*) the gas-phase enthalpies and entropies of binding X, Y and X–Y to a receptor, where the exothermicity of binding X–Y is taken as the sum of the exothermicities of X and Y when bound alone. Each binding event is represented by a vector from the origin to the relevant point on the enthalpy–entropy curve; dotted lines identify the relevant enthalpy and entropy terms on the *y* and *x* axes. In (*b*), the summation of the ***X*** and ***Y*** vectors are visualized. The difference in the entropic terms, corresponding to the binding of X–Y and the sum of the terms for X and Y, represents the chelate enhancement of binding ($T\Delta S°_{chelate}$). The vectors corresponding to the maximum possible chelate enhancement of binding, due to X and Y binding with large exothermicities and limiting adverse entropies, are represented in (*c*).

sum of its parts. Thus, $\Delta H°'_X$ and $\Delta H°'_Y$ represent the exothermicity of binding X and Y, respectively, when each is tethered to the other and $\Delta H°'_{X-Y}$ represents the total exothermicity of binding X–Y ($\Delta H°'_X + \Delta H°'_Y$). Hence, the co-operativity expressed as an increase in electrostatic bonding ($\Delta H°_{chelate}$) is distinct from, and expressed in addition to, the classical entropic chelate effect, $T\Delta S°_{chelate}$. The implications of this analysis are now illustrated experimentally.

Binding of the carboxylate group of cell-wall analogues to ristocetin A. The implication of the co-operativity expressed in Fig. 7 is that one functional group interaction between a ligand and a receptor can be improved electrostatically when additional interactions are introduced on the same template. Probably the best way to measure the exothermicity of an interaction is through the use of calorimetry, but cases where the binding of X, Y and X–Y can be measured with the necessary

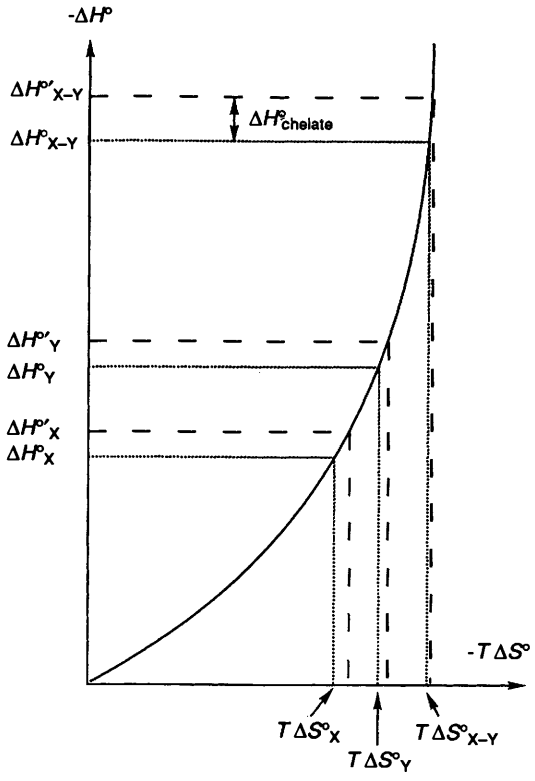

Fig. 7 Enthalpy–entropy curve illustrating co-operativity through the enthalpic benefit to binding when the electrostatic interactions of X are aided by Y, and Y by X, when the two are tethered together in X–Y. Dotted lines represent the enthalpies and entropies of binding X, Y and X–Y when the exothermicity of X–Y is taken to equal the sum of the exothermicities of the constituents parts, while the terms $\Delta H^{\circ\prime}_{X}$ and $\Delta H^{\circ\prime}_{Y}$ represent the numerically larger exothermicities of binding X and Y, respectively, when the binding of X and Y are mutually enhanced as part of X–Y. Thus, $\Delta H^{\circ}_{chelate}$ represents co-operativity expressed as an enhancement of electrostatic bonding.

precision are not readily available. An alternative approach is to infer the strength of a given electrostatic interaction by the measurement of proton NMR chemical shifts.[34] Thus when cell wall analogues RCO_2^- bind to ristocetin A, a member of the vancomycin group of antibiotics, the chemical shift of an amide NH w_2 (Fig. 8) is shifted appreciably downfield (> 3 ppm for tightly binding ligands) owing to the binding of the carboxylate anion to this NH. The magnitude of the downfield shift can be used as a measure of the strength of this electrostatic interaction. Larger binding shifts are taken to imply stronger electrostatic interactions in these complexes (as opposed to structural changes of different origin) since the carboxylate anion is a constant structural unit in a series of highly homologous ligands [Fig. 9(*a*)] that closely mimic the natural cell wall peptidoglycan recognition sequence -L-Lys-D-Ala-D-Ala. A corresponding set of chemical shift changes are also observed for the amide NH w_3 in the same carboxylate binding pocket. In Fig. 9(*b*), we plot the chemical shifts of w_2 and w_3, as the ligand containing the carboxylate group is extended to contain increasing numbers of ancillary groups [Fig. 9(*a*)], against the overall ligand binding energy measured at 298 K.[34] From these data it is apparent that the more extended ligands bind more strongly to the receptor antibiotic not only because the extending groups can add binding affinity, in the manner of a classical chelate effect, at a relatively small cost in entropy (since much of the exothermicity of binding comes from the interaction of the carboxylate group with three amide NHs), but also because these extending groups aid in holding the carboxylate anion more deeply in the electrostatic well which describes its interaction with the antibiotic. The data illustrate how multiple weak interactions on the same template act in a co-operative fashion to enhance the electrostatic binding energy of the carboxylate interaction.

We now illustrate the application of the general form of the curved enthalpy–entropy plot of Fig. 2 as an aid to the interpretation of the thermodynamic data on weak interactions in solution.

Enthalpy–entropy compensations for associations in solution. If two polar entities of solutes A and B interact (*e.g.*, through a hydrogen bond) to give a complex A.B, then if S is a solvent molecule then reaction (3) can be written. Each of the species in reaction (3) (A.S, B.S, A.B and S.S) are fully solvated; only

$$A.S + B.S \longrightarrow A.B + S.S \qquad (3)$$

interactions that are 'rearranged' in the association of A and B are indicated. We make the simplifying assumption that the magnitude of all other interactions with the solvent [that are treated implicitly in reaction (3)] are unaffected.

We consider associations involving a 'one-point' interaction, which we define as a weak but highly directional bond between associating species, rather than packing between van der Waals surfaces, for example. Although this definition is itself rather imprecise, it is a device which is fruitfully and frequently used in chemistry, *e.g.* the depiction (usually by a dotted line) of one (*versus* several) hydrogen bonds in an association [Scheme 2(*a*)], the specification of the interaction of a ligand to a metal,

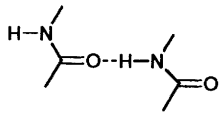

a

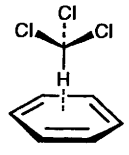

b

Scheme 2

or even the making of one 'hydrogen bond' between the C–H group of a chloroform molecule and the π-electron density on the face of a benzene ring [Scheme 2(*b*)].

In reaction (3), the following 'one-point' interactions are broken

$$A.S + B.S \longrightarrow A + B + S + S \qquad (4)$$

and the following 'one-point' interactions are made

$$A + B \longrightarrow A.B \qquad (5)$$

$$S + S \longrightarrow S.S \qquad (6)$$

In reactions (4) and (5), implicit solvation of A and B is assumed except at the point of interaction of A with B in A.B, or at the point of interaction of A or B with S in A.S or B.S. Similarly, in reactions (4) and (6), implicit solvation of S is assumed except at the explicit point of interaction with a second S molecule in S.S [reaction (6)], or with A or B in A.S or B.S.

All of the interactions made in reactions (5) and (6) will have an enthalpic benefit and an entropic cost (described in terms of $298\Delta S^{\circ}$ at 298 K); and the interactions broken [reaction (4)]

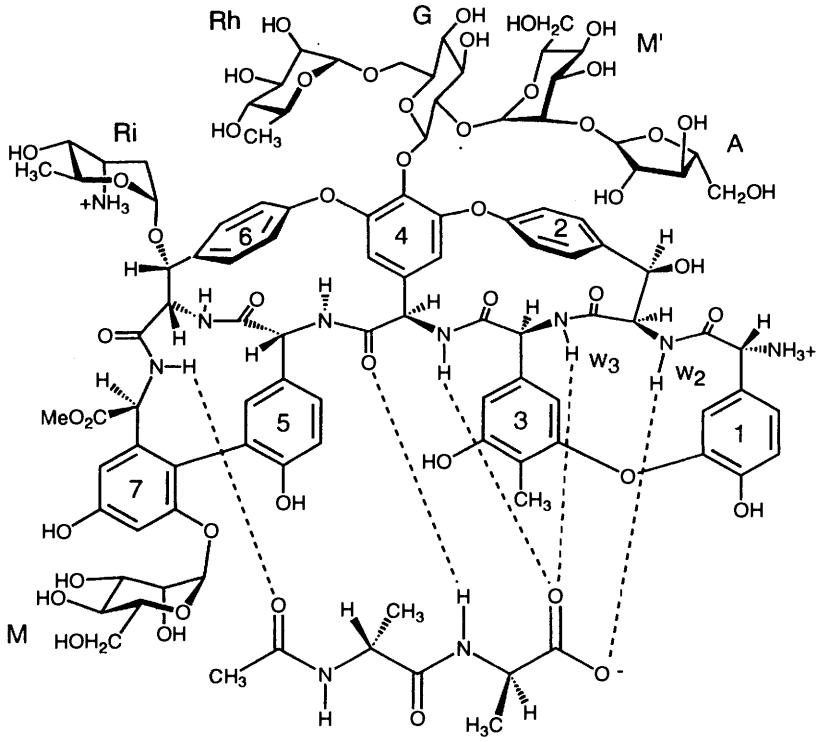

Fig. 8 Exploded view of the ristocetin A complex with the dipeptide cell wall analogue *N*-Ac-D-Ala-D-Ala. The amide NHs (w_2 and w_3) involved in binding the cell wall carboxylate anion are labelled; dotted lines represent intermolecular hydrogen bonds.

will have an enthalpic cost and an entropic benefit. Interactions represented in the upper right-hand quadrant of Fig. 10, with negative $\Delta H°$ values, correspond to bonds made [reactions (5) and (6)], and those in the identical, but inverted and reflected curve (lower left-hand quadrant), with positive $\Delta H°$ values, represent bonds broken [reaction (4)]. Each interaction corresponds to a point on the enthalpy–entropy compensation curve and is represented by a vector (solid line) from the origin to the point on the curve of Fig. 10. The net enthalpy and entropy terms, represented by the summation of the four vectors, give a guide to the overall Gibbs energy of association. The use of a single enthalpy–entropy compensation curve to describe all the interactions is of course a gross approximation, but we believe it is a useful one, and attempt in the following to show that it gives physical insight which may be useful.

The net enthalpy–entropy compensation (asterisk, Fig. 10) provides a value corresponding to the experimental data points appearing in Fig. 5 (for 'one-point' interactions). The data in Fig. 5 follow eqn. (7).

$$\Delta H° \approx 1.59\,(300\Delta S°)\ (r = 0.92) \qquad (7)$$

While the details of the relative magnitudes of the vectors is uncertain, it is evident that a net negative $\Delta H°$ value for association in solution indicates that for the enthalpic components of the vectors ***1***, ***2***, ***3*** and ***4*** in Fig. 10 (see key to vectors on Figure), it must be the case that ***1*** + ***2*** > ***3*** + ***4***. Fig. 10 illustrates one way of achieving this. It can be seen that a relatively large exothermicity for vector ***1*** is a feature of the experimental results summarized in Fig. 5 in cases where there is a large net exothermicity of association in solution. However, more competitive solute–solvent interactions lead to the expected decrease in the extent of association of A and B in solution. For example, interactions between secondary amides (Scheme 3) have been widely investigated in a variety of solvents revealing decreasing degrees of aggregation within the series CCl_4 > C_6H_6 > $CHCl_3, CH_2Cl_2$ > dioxane > water.[35] Similarly, the lactam, pyrrolidin-2-one forms a stable hydrogen-bonded dimer in CCl_4 ($K_{dim} \approx 10^2$ dm^3 mol^{-1}), but the association constant is substantially smaller in $CHCl_3$ (< 10 dm^3 mol^{-1});[36–38] the decrease in K_{dim} can be attributed to a selective increase in the extent of solvation of the unbound lactam. The association of lactams to form dimers (*e.g.* Scheme 3) is particularly exothermic in cyclohexane ($\Delta H° = -37$ kJ mol^{-1}),[37] where the solvent–solute interactions are presumably very weak (in accord with the limited solubility of these compounds in this solvent). In CCl_4, solute–solvent interactions are more competitive with lactam dimerization with net $\Delta H°$ values for association estimated to be between −18 and −28 kJ mol^{-1}.[37] The effects of relative solvation energies have been used in host–guest recognition studies to illustrate how major variations in association constants can be achieved through subtle changes in solvent structure and size.[17,36] We emphasize that it is not our intention in the current paper to present a detailed quantification of all of the variables presented in the above equations, but to highlight principles. Parameters for intermolecular interactions may become available through a factorization of experimental solvation data such as through a group additivity scheme,[39–41] or through computational approaches.[42–45]

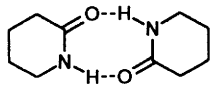

Scheme 3

With reference to Fig. 5, it is important to note that equilibrium constants for one-point associations in the range, say 10^3–10^4 dm^3 mol^{-1} ($\Delta G° \approx -20$ kJ mol^{-1}), could be achieved equally well by many other relationships between $\Delta H°$ and $T\Delta S°$, such as $\Delta H° \approx -30$ kJ mol^{-1} and $T\Delta S° \approx -10$ kJ mol^{-1}, or $\Delta H° \approx -20$ kJ mol^{-1} and $T\Delta S° \approx 0$ kJ mol^{-1}. In practice, this is not the case: despite the large number of variables involved, $\Delta H°$ and $T\Delta S°$ are described by the linear relationship given by eqn. (5), for which $\Delta G° \approx -20$ kJ mol^{-1} is

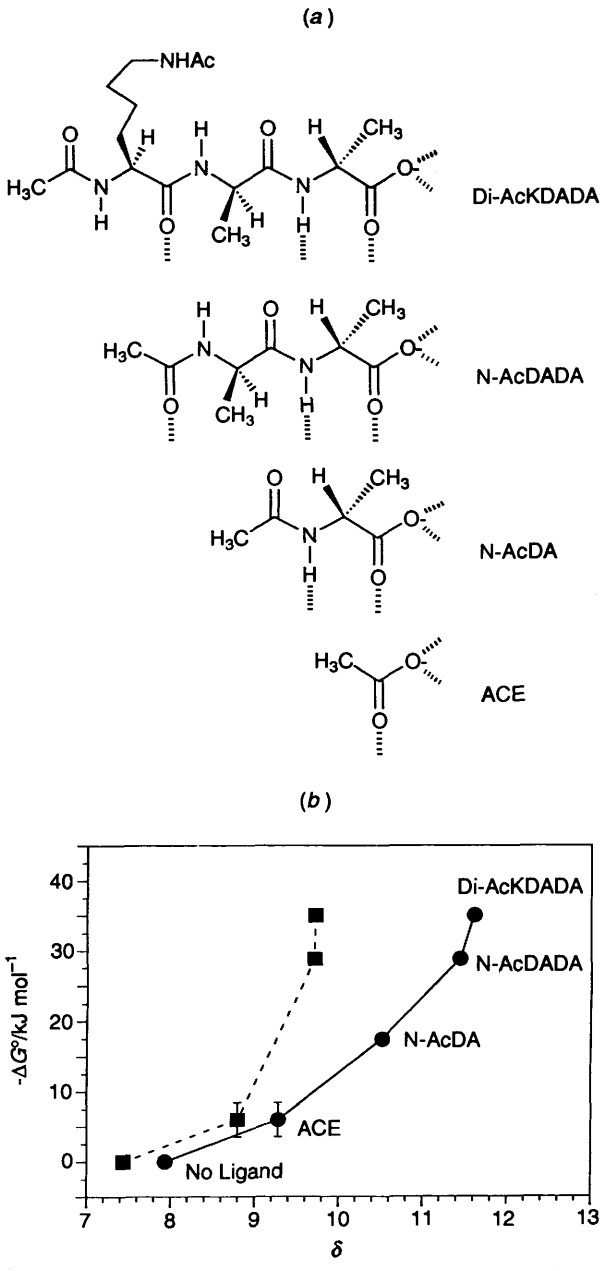

Fig. 9 (*a*) Structure of cell-wall analogues used in binding studies with ristocetin A. Hashed lines represent the position of hydrogen bonds to the antibiotic. (*b*) Plot of ligand binding energy ($\Delta G°$ at 298 K) *vs.* limiting chemical shift of antibiotic amide NHs w_2 and w_3 (pH 4.5). ^1H Chemical shifts were determined at 400 and 500 MHz and are referenced to internal trimethylsilylpropanoic acid. In all cases the w_2 and w_3 resonances are assigned on the basis of 2D NOE experiments (unpublished results). Error bars for ligand binding energies and chemical shift values lie within the size of the data point, except in the case of the binding of the acetate anion (ACE) where the uncertainty in $\Delta G°$ is indicated.

satisfied by $\Delta H° \approx -50$ kJ mol^{-1} and $T\Delta S° \approx -30$ kJ mol^{-1}. If one-point associations with negative $\Delta H°$ values always result in negative $T\Delta S°$ values in non-polar solvents, how then is entropy-driven binding achieved?

Entropy-driven association of two large discs: release of multiple solvent molecules. The previous section has focused on generalized physical details of processes where enthalpic benefit is greater than entropic cost. However, entropy-driven binding is a well known phenomenon;[46-50] how can the model help in understanding this phenomenon? We illustrate the consequences of Fig. 2 for the dimerization of two large discs where large surfaces are brought into contact with the release of a number of solvent molecules [Fig. 11(*a*)]. In such cases the association is not well approximated by one or two 'one-point' interactions. The eqns. (8)–(10) are now relevant: [again,

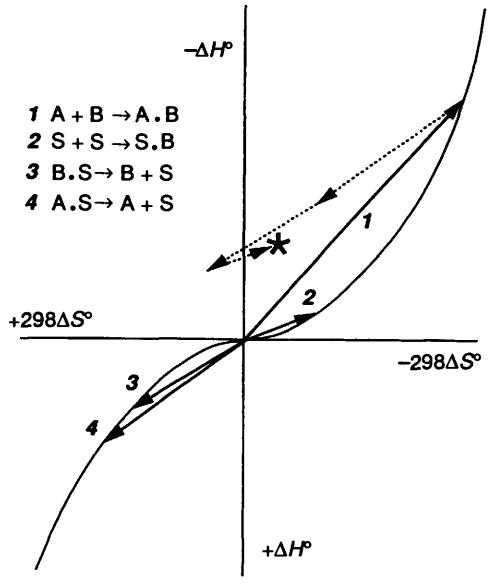

Fig. 10 Vector diagram describing contributions to 'one-point' associations in non-polar solvents. Each interaction (solute–solute, solute–solvent and solvent–solvent) is represented by a vector (see key on Figure) from the origin to the relevant point on the enthalpy *vs.* entropy curve. The net $\Delta H°$ and $300\Delta S°$ value (marked by an asterisk) is obtained by summing all vectors. Dotted lines enable the summation process to be visualized.

$$A + A \longrightarrow A.A \quad (8)$$

and

$$A.S_n + A.S_n \longrightarrow 2A + 2nS \quad (9)$$

$$2nS \longrightarrow nS.S \quad (10)$$

solvation is considered implicitly (see above) and only interactions that are rearranged during the association of two A molecules are highlighted].

The enthalpies corresponding to eqns. (8)–(10) are $\Delta H°_{A.A}$, $2n\Delta H°_{A.S}$, and $n\Delta H°_{S.S}$ and a situation is considered where $-\Delta H°_{A.S} \approx -2\Delta H°_{S.S}$ (*i.e.* a solvent molecule interacts more strongly with the solute molecule than with another solvent molecule) and $\Delta H°_{A.A}$ (solute–solute interaction) is much more exothermic than solvent–solvent or solvent–solute interactions [Fig. 11(*b*)]. The overall sign of $\Delta H°$ for the association [eqn. (11)] now depends not mainly on $\Delta H°_{A.A}$ (as it does for a 'one-

$$2A.S_n \longrightarrow A.A + nS.S \quad (11)$$

point' association in a non-polar medium), but also strongly on the sum of the number of solute–solvent interactions broken ($2n\Delta H°_{A.S}$) and the number of solvent–solvent interactions formed ($n\Delta H°_{S.S}$), hence:

$$\Delta H° = \Delta H°_{A.A} + n\Delta H°_{S.S} - 2n\Delta H°_{A.S} \quad (12)$$

For $-\Delta H°_{A.S} \approx -2\Delta H°_{S.S}$ the overall association becomes endothermic ($\Delta H° \geqslant 0$) for the release of n solvent molecules, when

$$n \geqslant 2/3\,(\Delta H°_{A.A}/\Delta H°_{A.S}) \quad (13)$$

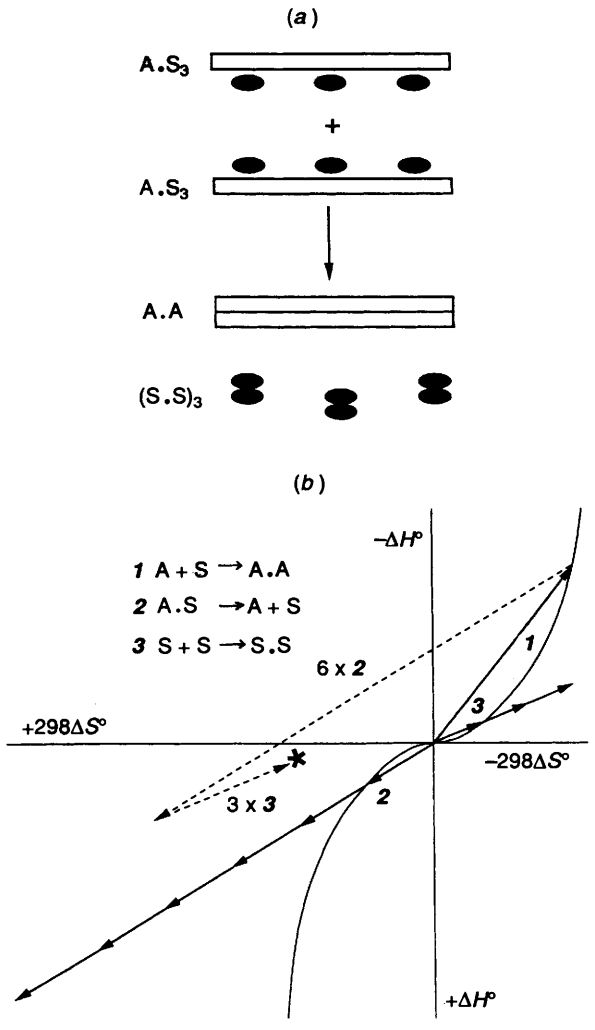

Fig. 11 (*a*) Schematic representation of the association of two disks of A to form an A.A dimer, with the release of a number of solvent molecules (black dots) that associate to form solvent dimers. For ease of illustration, we consider the release of three solvent molecules per monomer of A (six in total), which associate to give three solvent–solvent dimers. (*b*) Enthalpy–entropy compensation plots, corresponding to bond making (upper right hand quadrant) and bond breaking events (lower left quadrant), where each interaction is represented by a vector from the origin to a point on the curve (see key on Figure). Solvent–solute interactions *2* must be considered as six individual interactions, with the net vector displaced from the compensation curve (lower quadrant). Similarly, three vectors, corresponding to the formation of three solvent dimers *3*, are also represented (top quadrant) by a net vector displaced from the curve; a single vector *1* represents the A.A interaction. Summation of all interactions (visualized by the dotted lines) results in a net (small) endothermicity of association, but a large favourable entropy of association primarily as a consequence of the entropic advantage of release of solute-ordered solvent molecules back to the more disordered state of bulk solvent.

Such a case is considered for the breaking of six solvent interactions to 2A molecules and the making of three new solvent–solvent associations and the A.A associated state, as shown in Fig. 11(*a*). Each of the contributing terms is represented by a vector in Fig. 11(*b*) and illustrates how overall such an association can be endothermic and yet give a large binding constant for an entropy driven association. To reiterate, the lower curve in Fig. 11(*b*) represents bond-breaking events ($\Delta H°$ +ve, $T\Delta S°$ +ve); the upper curve bond-making interactions ($\Delta H°$ −ve, $T\Delta S°$ −ve). The breaking of two solvent–solute interactions and formation of one solvent–solvent interaction must be considered three times. In Fig. 11(*b*), the case is illustrated where the A + S association is approximately twice as exothermic as the S + S association. The asterisk in Fig. 11(*b*) indicates the net $\Delta H°$ and $T\Delta S°$ values for association in solution and hence the net $\Delta G°$ for association. The position of the asterisk indicates that the net enthalpy of association is small, but that the entropy term is large and positive and provides the driving force for association. Thus, the curvature of the enthalpy–entropy plot for a given interaction, in combination with the breaking of multiple interactions on one template provides the basis for the entropy-driven binding mechanism.

Table 1 Thermodynamic data for the formation of complex ions of polyamines in aqueous solution (data from Dasent)[51]

	$\Delta H°_{298}$	$T\Delta S°_{298}$	$\Delta G°_{298}$
Mn[a]	−12.6	20.7	−33.3
Fe[a]	−26.4	23.1	−49.5
Ni[a]	−63.4	27.5	−90.9
Mn[b]	−25.2	2.5	−27.7
Fe[b]	−43.5	0	−43.5
Ni[b]	−76.4	3.8	−80.2

[a] $M(H_2O)_6^{2+}$ (aq) + tren (aq) ⟶ $M(tren)(H_2O)_2^{2+}$ (aq) + $4H_2O$ (l). [b] $M(H_2O)_6^{2+}$ (aq) + 2en (aq) ⟶ $M(en)_2(H_2O)_2^{2+}$ (aq) + $4H_2O$ (l).

The association of two discs with large solvated surface areas (as described above) is exemplified by the 'lock and key' velcraplex dimers and hemicarceplex complexes reported by Cram and co-workers.[46,47] The authors propose that numerous solvent (chloroform) molecules are liberated in the association, making the net process entropically favourable and in a number of examples enthalpically unfavourable (range of $\Delta H°$ values *ca.* −30 to +20 kJ mol^{-1}).

We next apply the model to some associations which show the unusual property of being more favourable in entropy terms as the interaction becomes markedly more exothermic.

Binding with more net bonding but less net order: metal chelation by polyamines. We illustrate this case for water as solvent. In such cases, the release of a water molecule from the metal ion prior to amine association will be endothermic and the release will be accompanied by a favourable change in entropy (due to its now greater motion in bulk solvent). Since the desolvation of the metal ion in water should be associated with a relatively large positive enthalpy change, the associated favourable entropy change would have to be read off from a relatively high positive $\Delta H°$ value in Fig. 2. This situation is relevant to the binding of a polyamine ligand to a series of metal ions, where the series of metal ions binds both water molecules and each of the amino groups of the polyamine with increasingly favourable $\Delta H°$ upon passing along the series of metal ions. For example, in the association of 2,2′,2″-triaminoethylamine [tren = $N(CH_2CH_2NH_2)_3$], or ethylenediamine [en = $(CH_2NH_2)_2$], to the series of metals Mn^{2+}, Fe^{2+} and Ni^{2+}. The relevant data are given in Table 1.[51] The stronger binding of nitrogen lone-pair donating ligands relative to oxygen lone-pair donating ligands (specifically water) is indicated by the exothermicities of the associations in Table 1; and the increasing difference in this binding on passing along the series $Mn^{2+} \rightarrow Fe^{2+} \rightarrow Ni^{2+}$ is indicated by the increasing exothermicity. That this increase reflects both the binding of the amine and water ligands is suggested by the decreasing rate constants (s^{-1}) for substitution of inner-sphere water molecules passing along the metal ion series in the same direction ($10^{7.5}$ *vs.* $10^{6.7}$ *vs.* $10^{4.5}$ s^{-1}).[52]

We now analyse the data of Table 1 and in so doing, consider the various steps of ligand–metal ion association, water–water association, ligand–water dissociation and metal ion–water

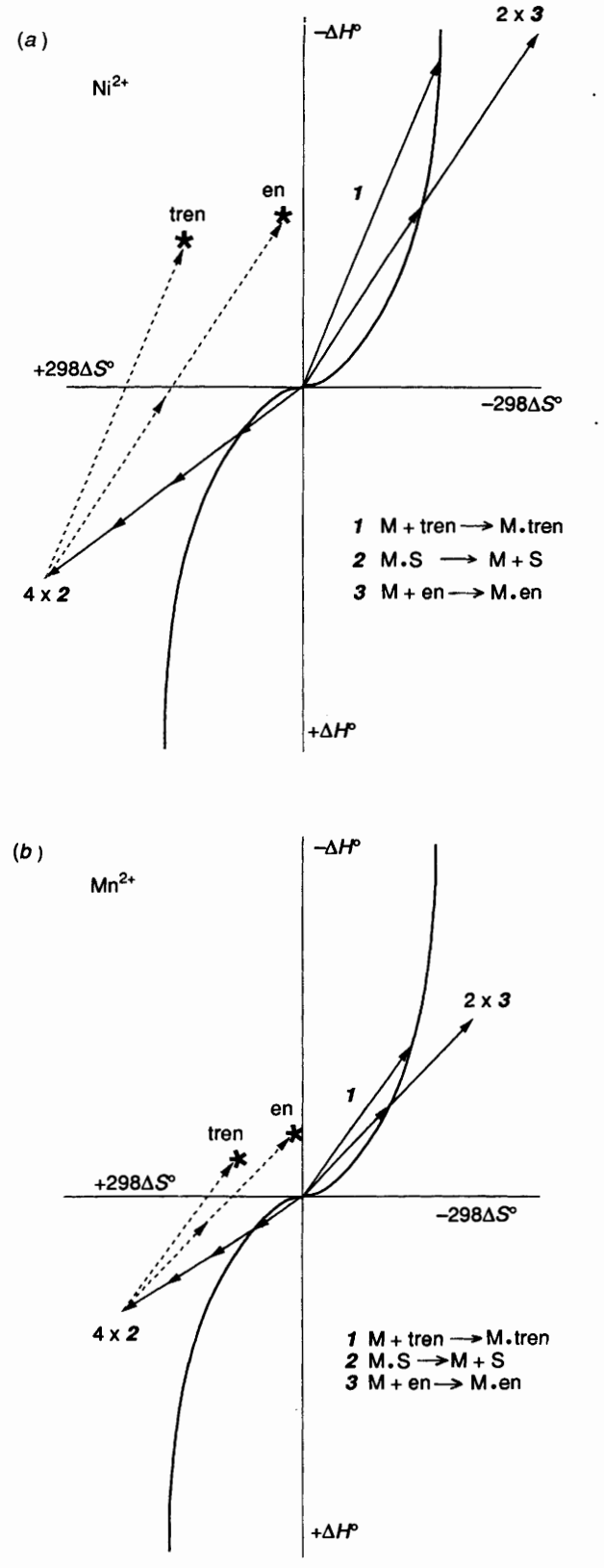

Fig. 12 Vector diagrams representing the various events leading to polyamine associations with metal ions in water. Associations are considered for Ni^{2+} (*a*) and Mn^{2+} (*b*) complexing with the polyamine ligands tren and en (see text). The key to vector numbering is found on the figure; M represents divalent metal ion (Mn^{2+} or Ni^{2+}) and S a solvent molecule.

dissociation as isolated events occurring in the aqueous medium. The relevant considerations are: (*i*) As we pass along the series of metals which binds the polyamine more and more strongly ($Mn^{2+} < Fe^{2+} < Ni^{2+}$), the binding of the four amino groups of the tren ligand is so strongly exothermic that the cost in entropy within the series does not increase very much (*i.e.* all values are taken from high in the top right hand quadrant of Fig. 12). These vectors will have increasing slopes $d(-\Delta H°)/d(-T\Delta S°)$ through the progression $Mn^{2+} \rightarrow Fe^{2+} \rightarrow Ni^{2+}$ and are labelled *1* in the plots for Ni^{2+} [Fig. 12(*a*)] and Mn^{2+} [Fig. 12(*b*)]. (*ii*) Approximately four water molecules will be lost from the metal ions to allow the binding described under (*i*) to occur. However, since (unlike the amino groups) the water molecules are not on one template, the four vectors which determine the entropic benefit of these losses (relative to the enthalpic cost) will be inclined at a less steep angle (relative to the $T\Delta S°$ axis) than the vector for tetraamine association. For example, in qualitative terms, the process of tetraamine association to Ni^{2+} could be represented by vector *1* and that of water dissociation by vector *2*. This is because the endothermicity per mole of water lost is much less than the exothermicity per mole of tetraamine gained. The vector for loss of water from the metal ions must be considered $\times 4$, with a consequently large benefit in entropy [these vectors for Ni^{2+} and Mn^{2+} are labelled *2* in Figs. 12(*a*) and 12(*b*)]. More importantly in the present context, the water vector will increase its slope $d(|\Delta H°|)/d(|T\Delta S°|)$ as the change $Mn^{2+} \rightarrow Fe^{2+} \rightarrow Ni^{2+}$ is made. Since we are operating in a region where $d(|\Delta H°|)/d(|T\Delta S°|)$ for the water dissociation is smaller than for the tetraamine association, as we pass along the series of metals the entropic benefit of water loss will increase more rapidly than the entropic cost of tetraamine association. Thus, as the exothermicity of the tetraamine complex formation increases, the entropy of complex formation becomes more favourable, in accord with the experimental facts (Table 1). Although existing models may be able to justify the data, Fig. 12 provides a clear understanding of the relative importance of the processes at work. If Fig. 12 were to be used to give a qualitative insight into the absolute magnitudes of the thermodynamic data presented in Table 1, then the vectors shown there for the processes involving the metal ions would have to be added together along with those for the related water–water associations and the ligand–water dissociations. However, in the present context, the water–water associations and the ligand–water dissociations can perhaps usefully be taken as cancelling each other and, therefore, are omitted from the analysis.

We now turn to the data for the ethylenediamine complexes (Table 1). In these cases, the vector for diamine–metal association has a smaller $d(|\Delta H°|)/d(|T\Delta S°|)$ slope than for tetraamine association (only about half the exothermicity), but must be considered twice (two moles associate). The relevant vectors for Ni^{2+} and Mn^{2+} are marked *3* in Fig. 12(*a*) and 12(*b*), respectively. The consequence is that the increased adverse entropy term in binding two moles of en on passing from Mn^{2+} to Ni^{2+} is larger than in binding one mole of tren. Despite this, the en ligand can still associate with greatly increased exothermicity in the series $Mn^{2+} \rightarrow Fe^{2+} \rightarrow Ni^{2+}$ without an adverse increase in entropy (Table 1). This is again a consequence of the fact that increased exothermicity expressed on a multiply bound template is less costly in entropy than is increased exothermicity on a number of separately bound ligands. This effect is apparent from a consideration of the magnitude of the chelate effect as a function of the exothermicity of the associated interactions.

Conclusions

Linear correlations between enthalpy and entropy have previously been observed,[9–24] but a unifying description of the origin of the effect has not emerged. In this paper experimental data and theoretical considerations have been used to illustrate

the general form of an entropy–enthalpy compensation curve, and to highlight its utility in presenting a description of various binding phenomena in solution (with restriction to a temperature of 298 K and molecular masses in the range *ca.* 100–300 Da). We appreciate that the shape of the curve is dependent upon many variables and is, as yet, a somewhat crude approximation. However, the utility of the curve in understanding the basis of phenomena such as co-operativity, entropy-driven binding and aspects of complexation of metal cations by multidentate ligands in aqueous solution, illustrate its value and potential.

Acknowledgements

We thank GLAXO (UK), EPSRC and BBSRC (UK) and Fisons (UK) for financial support. We are grateful to Dr. Richard Bonar-Law for helpful discussions.

References

1 M. I. Page and W. P. Jencks, *Proc. Natl. Acad. Sci. U.S.A.*, 1971, **68**, 1678.
2 P. R. Andrews, D. J. Craik and J. L. Martin, *J. Med. Chem.*, 1984, **27**, 1648.
3 A. J. Doig and D. H. Williams, *J. Am. Chem. Soc.*, 1992, **114**, 338.
4 M. S. Searle and D. H. Williams, *J. Am. Chem. Soc.*, 1992, **114**, 10 690.
5 W. P. Jencks, *Adv. Enzymol.*, 1975, **43**, 219.
6 W. P. Jencks, *Proc. Natl. Acad. Sci. U.S.A.*, 1981, **78**, 4046.
7 D. H. Williams, M. S. Searle, J. P. Mackay, U. Gerhard and R. A. Maplestone, *Proc. Natl. Acad. Sci. U.S.A.*, 1993, **90**, 1172.
8 D. H. Williams, M. S. Searle, M. S. Westwell, U. Gerhard and S. E. Holroyd, *Philos. Trans. R. Soc. London, A*, 1993, **345**, 11.
9 Y. Inoue, T. Hakushi and Y. Liu, in *Cation Binding by Macrocycles*, eds. Y. Inoue and G. W. Gokel, Marcel Dekker, New York, 1990, ch. 1.
10 Y. Inoue and T. Hakushi, *J. Chem. Soc., Perkin Trans. 2*, 1985, 935.
11 Y. Inoue, T. Hakushi, Y. Liu, L.-H. Tong, J. Hu, G.-D. Zhao, S. Huang and B.-Z. Tian, *J. Phys. Chem.*, 1988, **92**, 2371.
12 Y. Liu, L.-H. Tong, S. Huang, B.-Z. Tian, Y. Inoue and T. Hakushi, *J. Phys. Chem.*, 1990, **94**, 2666.
13 Y. Inoue, F. Amano, N. Okada, H. Inada, M. Ouchi, A. Tai, T. Hakushi, Y. Liu and L.-H. Tong, *J. Chem. Soc., Perkin Trans. 2*, 1990, 1239.
14 Y. Liu, L.-H. Tong, Y. Inoue and T. Hakushi, *J. Chem. Soc., Perkin Trans. 2*, 1990, 1247.
15 Y. Inoue, T. Hakushi, Y. Liu, L.-H. Tong, B.-J. Shen and D.-S. Jin, *J. Am. Chem. Soc.*, 1993, **115**, 475.
16 Y. Aoyama, M. Asakawa, Y. Matsui and H. Ogoshi, *J. Am. Chem. Soc.*, 1991, **113**, 6233.
17 D. B. Smithrud, T. B. Wyman and F. Diederich, *J. Am. Chem. Soc.*, 1991, **113**, 5424.
18 M. S. Searle and D. H. Williams, *Nucl. Acids Res.*, 1993, **21**, 2051.
19 M. R. Eftink, A. C. Anusiem and R. L. Biltonen, *Biochemistry*, 1983, **22**, 3884.
20 J. Becvar and G. Palmer, *J. Biol. Chem.*, 1982, **257**, 5607.
21 R. Lumry and S. Rajender, *Biopolymers*, 1970, **9**, 1125.
22 W. C. Conner, Jr., *J. Catal.*, 1982, **78**, 238.
23 J. E. Leffler, *J. Org. Chem.*, 1955, **20**, 1202.
24 W. Linert and R. F. Jameson, *Chem. Soc. Rev.*, 1989, **18**, 477.
25 R. U. Lemieux, L. T. Delbaere, H. Beierbeck and U. Spohr, *Host–Guest Molecular Interactions from Chemistry to Biology*, Ciba Foundation Symposium; Wiley, Chichester, 1991, pp. 231–238.
26 C. J. Biermann, *Indian J. Chem.*, 1988, 855.
27 *CRC Handbook of Chemistry and Physics*, CRC Press Inc., Boston, MA, 1991, 72nd edn.
28 P. W. Atkins, *Physical Chemistry*, Oxford University Press, London, 1982, 4th edn.
29 J. K. Kochi, *Free Radicals*, Wiley, New York, 1973, vol. II.
30 M. Tamres, in *Molecular Complexes*, ed. R. Foster, Elek Science, London, 1973.
31 F. D. Rossini, D. D. Wagman, W. H. Evans, S. Levine and I. Jaffe, *Selected Values of Chemical Thermodynamic Properties*, National Bureau of Standards, Washington DC, 1952.
32 S. L. A. Adebayo, A. C. Legon and D. J. Millen, *J. Chem. Soc., Faraday Trans.*, 1991, **87**, 443.
33 R. Foster, *Organic Charge Transfer Processes*, Academic Press, London, 1969, and refs. therein.
34 P. Groves, M. S. Searle, M. S. Westwell and D. H. Williams, *J. Chem. Soc., Chem. Commun.*, 1994, 1519.
35 W. L. Jorgensen, *J. Am. Chem. Soc.*, 1989, **111**, 3770.
36 K. T. Chapman and W. C. Still, *J. Am. Chem. Soc.*, 1989, **111**, 3075.
37 J. A. Walmsley, E. J. Jacob and H. B. Thompson, *J. Phys. Chem.*, 1976, **80**, 2745.
38 G. Montaudo, S. Caccamese and A. Recca, *J. Phys. Chem.*, 1975, **79**, 1554; S. E. Krikorian, *J. Phys. Chem.*, 1982, **86**, 1875.
39 W. K. Stephenson and R. Fuchs, *Can. J. Chem.*, 1985, **63**, 2529.
40 W. K. Stephenson and R. Fuchs, *Can. J. Chem.*, 1985, **63**, 2535.
41 V. N. Levchuk, I. A. Khachikov, I. I. Sheikhet and B. Ya. Simkin, *Zh. Obshch. Khim.*, 1990, **60**, 1193.
42 W. L. Jorgensen and J. Tirado Rives, *J. Am. Chem. Soc.*, 1988, **110**, 1657.
43 W. L. Jorgensen, J. M. Briggs and M. L. Contreras, *J. Phys. Chem.*, 1990, **94**, 1683.
44 W. L. Jorgensen and D. L. Severance, *J. Am. Chem. Soc.*, 1990, **112**, 4768.
45 J. Pranata, S. G. Wierschke and W. L. Jorgensen, *J. Am. Chem. Soc.*, 1991, **113**, 2810.
46 D. J. Cram, H.-J. Choi, J. A. Bryant and C. B. Knobler, *J. Am. Chem. Soc.*, 1992, **114**, 7748.
47 D. J. Cram, M. T. Blanda, K. Paek and C. B. Knobler, *J. Am. Chem. Soc.*, 1992, **114**, 7765.
48 T. K. Chandrashekar and V. Krishnan, *Inorg. Chim. Acta*, 1982, **62**, 259.
49 T. K. Chandrashekar and V. Krishnan, *Bull. Soc. Chim. Fr., Part 1*, 1984, 42.
50 R. M. Izatt, J. S. Bradshaw, K. Pawlak, R. L. Bruening and B. J. Tarbet, *Chem. Rev.*, 1992, **92**, 1261.
51 W. E. Dasent, *Inorganic Energetics—An Introduction*, Cambridge University Press, Cambridge, 1982, 2nd edn., p. 175.
52 F. A. Cotton and G. Wilkinson, *Advanced Inorganic Chemistry*, Wiley, New York, 1989, 5th edn., p. 1289.

Paper 4/03341H
Received 6*th June* 1994
Accepted 30*th August* 1994